
Rethinking Spiking Neural Networks as State Space Models

Malyaban Bal
The Pennsylvania State University
University Park, PA 16802
mjb7906@psu.edu

Abhronil Sengupta
The Pennsylvania State University
University Park, PA 16802
sengupta@psu.edu

Abstract

Spiking neural networks (SNNs) are posited as a biologically plausible alternative to conventional neural architectures, with their core computational framework resting on the extensively studied leaky integrate-and-fire (LIF) neuron design. The stateful nature of LIF neurons has spurred ongoing discussions about the ability of SNNs to process sequential data, akin to recurrent neural networks (RNNs). Despite this, there remains a significant gap in the exploration of current SNNs within the realm of long-range dependency tasks. In this study, to extend the analysis of neuronal dynamics beyond simplistic LIF mechanism, we present a novel class of stochastic spiking neuronal model grounded in state space models. We expand beyond the scalar hidden state representation of LIF neurons, which traditionally comprises only the membrane potential, by proposing an n -dimensional hidden state. Additionally, we enable fine-tuned formulation of neuronal dynamics across each layer by introducing learnable parameters, as opposed to the fixed dynamics in LIF neurons. We also develop a robust framework for scaling these neuronal models to deep SNN-based architectures, ensuring efficient parallel training while also adeptly addressing the challenge of non-differentiability of stochastic spiking operation during the backward phase. Our models attain state-of-the-art performance among SNN models across diverse long-range dependency tasks, encompassing the Long Range Arena benchmark, permuted sequential MNIST, and the Speech Command dataset. Moreover, we provide an analysis of the energy efficiency advantages, emphasizing the sparse activity pattern intrinsic to this spiking model.

1 Introduction

Spiking neural networks (SNNs) [1] have garnered attention as a compelling bio-plausible substitute for traditional artificial neural networks (ANNs). Their appeal stems from their utilization of spike-based communication among neurons, a feature that closely mimics biological processes. Additionally, the inherent stateful nature of SNNs enables them to adeptly handle temporal information [2], further enhancing their suitability for various applications. The sparse spike-based information flow characteristic of SNNs facilitates event-driven computation and communication in neuromorphic hardware, leading to substantial energy savings [3]. SNN-based models, ideal for edge computing, have undergone rigorous testing on neuromorphic hardware platforms such as Intel Loihi 2 [4], IBM TrueNorth [5], among others showcasing orders of magnitude improvements in energy efficiency.

In the progression of SNN-based architecture advancements, research has predominantly focused on employing leaky-integrate-and-fire (LIF) neurons [6]. While the dynamics modeled by LIF neurons are deemed biologically plausible, the actual operations within the brain entail additional layers of complexity [7] and stochasticity [8] that are not fully captured by the simplified LIF neuron model. Moreover, this inherent constraint has hindered the widespread adoption of spiking neural architectures for tasks involving long-range dependencies. Some existing approaches that apply SNNs

to sequential data, albeit on a limited sequence length, resort to more computationally expensive and biologically implausible operations, such as attention mechanisms [9, 10]. In this paper, we harness the intrinsic dynamics of our proposed spiking neuronal model to tackle previously unexplored long-range dependency tasks within the realm of spiking neural architectures.

State Space Models (SSMs) serve as fundamental scientific models utilized across various disciplines, notably in control theory, to articulate the behavior of dynamic systems. SSMs offer a streamlined and robust framework, facilitating a comprehensive analysis and deep understanding of the dynamics of complex systems as they unfold over time. Recently, SSMs have been employed in traditional non-spiking architectures to effectively model sequence learning tasks [11]. Moreover, they have demonstrated comparable performance to transformer-based architectures while demanding significantly fewer computational resources [12]. Since, SSMs are not constrained by the quadratic complexity of mechanisms like vanilla attention mechanism [13], they can be scaled effectively to accommodate long sequences.

In this paper, we introduce a novel class of neuronal models called **Stochastic Spiking Structured State Space Models (S6)**. These models build upon the neuronal dynamics observed in biological neurons by incorporating inherent stochastic characteristics. Moreover, diverging from the conventional representation of the hidden state—typically a scalar, such as the membrane potential in LIF neurons—we enhance the information encoding capacity of each neuron by formulating an n -dimensional hidden state. The dynamics of each neuron can be learned through an independent set of governing parameters, thereby enhancing the capacity of the model to process different temporal dependency patterns across different neurons.

To leverage S6-based neuronal layers for complex long-range dependency tasks, this paper aims to develop a scalable architecture and robust training framework. Adhering to general SNN dynamics, communication between each layer relies on spikes, eliminating floating-point matrix multiplication operations in our architecture, particularly during inference. This design along with sparse neuronal activity significantly enhances the energy/power efficiency of our model compared to conventional neural architectures of a similar scale. Moreover, to address the challenge of non-differentiability inherent in the stochastic spiking function, we introduce a novel surrogate in the form of $\mathbb{E}[S_t]$, where the discrete Bernoulli random variable S_t , associated with each neuron at time t , indicates whether the neuron has spiked or not. We demonstrate the effectiveness of our model through rigorous evaluation, surpassing the performance of traditional non-spiking transformer-based architectures on tasks with long-range dependencies. Additionally, our model sets a new benchmark for spiking architectures. Our evaluation spans across various datasets within the Long Range Arena (LRA) benchmark, along with sequence-based datasets such as permuted sequential MNIST (psMNIST) and the raw inputs of the SC10 subset of the Speech Command dataset.

The primary contributions of our work are as follows:

- **S6 Neuronal Model:** We propose a novel class of neuronal models which is characterized by an underlying structured state space model and a stochastic spiking output function. Unlike LIF neurons, the dynamics of individual S6 neurons, across different layers, can be fine-tuned by learning the underlying parameters during training.
- **S6-Based Scalable SNN Training Framework:** We develop a robust training framework for effectively scaling our S6-based SNN architectures. We introduce a SpikeSampling layer that, during the forward phase, generates spikes from each neuron based on the probability of random variable S_t at time t . We address the challenge of non-differentiability in the stochastic spiking operation during the backward phase by proposing a surrogate operation.
- **Application to Long-Range Dependency Tasks:** We evaluate the performance of our proposed S6-based model across multiple long-range dependency tasks like psMNIST, SC10 dataset, and the Long Range Arena (LRA) benchmark. Our model achieves state-of-the-art results compared to other spiking models and transformer-based non-spiking architectures. We also highlight the energy efficiency inherent in these models due to sparsity of spikes.

2 Related Works

Alternate SNN Formulations: While the majority of SNN studies [2, 10, 9] are grounded in the LIF neuron architecture, there is also research, albeit in a limited scale of application, exploring

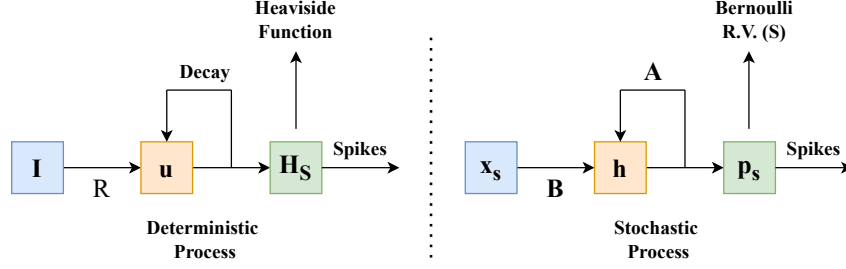


Figure 1: High-level overview of the underlying dynamics of a conventional LIF neuronal model (*left*) compared to our proposed S6 model (*right*). In contrast to the single-dimensional membrane potential $u[t]$ representing the hidden state in an LIF model at time t , our approach expands this concept to a higher-dimensional latent space $h[t]$, enhancing the capacity of the model to represent internal states across n -dimensions. Moreover, S6 models the spiking operation as a stochastic process, contrasting with the deterministic mechanism employed in LIF models.

alternative neuronal models, such as the Hodgkin-Huxley (HH) neuron [14], on neuromorphic systems like SpiNNaker [15], aiming to enhance the expressiveness of neuronal models. Previous literature has also delved into stochastic spiking neurons, largely within the confines of smaller vision-based datasets [16, 17]. The idea of dynamics thresholding which results in different hidden state dynamics has also been explored in the limited setting of image based datasets [18]. All of these efforts aim to enhance the expressiveness, biological plausibility, and energy efficiency of SNNs. Nevertheless, the scale of these prior endeavors has not yet reached the level required to address the extensive long-range dependency task investigated in this study.

Long-Range Dependency Modelling: The realm of sequence modeling is primarily dominated by transformer-based architectures. Efficient implementations like LinFormer [19], Performer [20], among others, have demonstrated scalability to long sequence lengths. Meanwhile, non-spiking architectures based on SSMs, such as S4 and Mamba [12, 11, 21], have also shown the capability to handle lengthy sequences. SNN-based architectures have primarily been applied to vision-based datasets [2, 9] and NLP datasets [10], typically with constrained sequence lengths. However, within the domain of SNNs, frameworks based on Legendre Memory Units (LMUs) [22, 23] has ventured into exploring long-range dependency tasks. One study [24] explores a spiking version of S4 model in a limited setting of speech datasets extending the output of S4 into an LIF layer.

3 Methodology

In this section, we first delve into the dynamics of vanilla LIF-based SNNs. Following that, we will construct the S6 neuronal model founded on SSMs, drawing insightful parallels (Fig. 1) with conventional LIF neurons. We will then proceed to delve into the architectural intricacies, providing detailed insights into how we can scale deep SNN models using S6 neurons as fundamental building blocks. Finally, we will embark on exploring a robust training framework tailored for our models.

3.1 Spiking Neural Networks

The core neuronal model in majority of SNN architectures is founded on the principles of LIF neurons. These neurons, closely mirroring biological counterparts, serves as a simplified bio-plausible abstraction of the underlying dynamics of biological neurons. Here, we examine the internal dynamics of a basic LIF neuron as outlined below,

$$\tau_m \cdot \frac{du}{dt} = -(u(t) - u_{rest}) + R \cdot I(t) \quad (1)$$

where, at time t , $u(t) \in \mathbb{R}$ is the membrane potential which can be considered as the hidden variable of the system, responsible for maintaining the state; $I(t)$ is the input current scaled by a constant, R , representing resistance; τ_m is the time constant which is associated with the decay in membrane potential over time, thus influencing internal dynamics; u_{rest} is the resting membrane potential.

Moreover, in a deterministic fashion, if $u > V_{th}$, then the neuron emits a spike, i.e., it sends out a ‘1’ else ‘0’ and its potential is reset. LIF-based SNNs are often likened to recurrent neural network (RNN) architectures for two primary reasons: firstly, they operate over a defined number of time steps, and secondly, unlike neurons in conventional networks, they possess inherent statefulness. Given that τ_m and u_{rest} are typically fixed hyper-parameters, meaning they are not learnt, the hidden state dynamics of LIF neurons remain consistent across all neuronal layers. In our work, we primarily focus on fine-tuned formulation of neuronal dynamics of each layer and generalizing the membrane potential usually given by a real-valued scalar to n -dimensional latent space of hidden variables. We also propose a stochastic spiking mechanism which is explained in more details in the next section.

3.2 Stochastic Spiking Structured State Space Models (S6)

In our paper, adhering to an SSM-based formulation, we introduce a novel class of neuronal models characterized by adaptive dynamics (through learnable parameters), increased hidden state representation and stochastic spiking operation. The main objective of this formulation is to reexamine the fundamentals of SNNs in a manner that is more generalizable and bio-plausible, rather than imposing specific constraints onto the system. This approach enables the development of a more scalable and energy-efficient spiking architecture.

3.2.1 S6 Formulation

We formulate the neuronal model as a time invariant system which takes in input spikes given as $x_s(t) \in \{0, 1\}$, at time t . Much like the membrane potential ($u(t)$) upholds the state of the LIF, we anchor our approach in SSMs [12, 11], crafting an n -dimensional hidden state ($h(t) \in \mathbb{R}^n$) at time t . Expanding the dimensionality of the hidden state enables our neuronal model to achieve a more comprehensive state encoding of the underlying input sequence, surpassing the limitations imposed by the scalar hidden state ($u(t)$ in Eqn. 1) in LIF models. The event of spike generation at time t is associated with Bernoulli random variable S_t corresponding to each neuron. The probability of spiking, i.e., $p_s(t)$ at time t , is modelled as the output of the neural model. The continuous time neuronal dynamics are expressed as,

$$\begin{aligned} \dot{h}(t) &= Ah(t) + Bx_s(t) \\ p_s(t) &= \sigma(CH(t) + Dx_s(t) \end{aligned} \quad (2)$$

where, $\dot{h}(t) = \frac{dh}{dt}$, A is a parameter controlling how the hidden state evolves over time without any input spikes. B represents the influence of the input spikes ($x_s(t)$). C describes how the hidden state vector $h(t)$ is mapped to the observed outputs, i.e., $p_s(t)$. D is the feedforward parameter, representing any direct influence of the inputs spikes $x_s(t)$ on the observed output probability $p_s(t)$. For the purpose of simpler formulation, following previous works [12], we will consider $D = 0$, since the term $Dx_s(t)$ can be viewed as a simple skip-connection. Furthermore, σ is a function that clips the output between $[0, 1]$, since probability $p_s[t] \in [0, 1]$. Thus, the learnable parameters can reformulate the neural dynamics during training, in contrast to the fixed decay-based dynamics determined by the limited hyper-parameters (such as τ_m and u_{rest}) of the LIF model. Furthermore, instead of the deterministic Heaviside function of LIF, we implement a biologically plausible stochastic spiking mechanism (Fig. 1). Given our focus on discrete time settings, particularly within domains like NLP and vision tasks, we now delve into formulating the dynamics of our neuronal model in discrete time.

3.2.2 S6 Discrete Time Dynamics

In order to discretize our system we sample a sequence of spikes of length L , given by $X_s = (x_s[1], x_s[2], \dots, x_s[L])$ from the original continuous signal given by $x_s(t)$, with step size Δ such as $x_s[i] = x_s(i\Delta)$. The S6 neuronal dynamics are subsequently discretized using bilinear transformations [25], whereby we approximate the parameters A, B, C as $\bar{A}, \bar{B}, \bar{C}$ which is given as,

$$\begin{aligned} \bar{A} &= (I - \Delta/2 \cdot A)^{-1}(I + \Delta/2 \cdot A) \\ \bar{B} &= (I - \Delta/2 \cdot A)^{-1}\Delta B \\ \bar{C} &= C \end{aligned} \quad (3)$$

where, I is the Identity matrix. The transition dynamics of the discretized system at time step t is,

$$\begin{aligned} h[t] &= \overline{A}h[t-1] + \overline{B}x_s[t] \\ p_s[t] &= \sigma(\overline{C}h[t]) \end{aligned} \quad (4)$$

where, $h[t]$ is the hidden state of the neuron, $p_s[t]$ is the probability of the event S_t . This allows us to write the transition dynamics of the system as a recurrence in discrete time.

Now, instead of using a recurrent representation, we investigate how the evolution of state dynamics can be represented by a convolution operation (with spikes as input signal), thereby completely circumventing floating-point tensor multiplications during inference. Moreover, employing convolution instead of a recurrence-based approach enables us to accelerate and parallelize the training process.

3.2.3 Representing Dynamics as Convolution over Spikes

There are two problems with Eqn. 4, concerning the training of a scalable spiking architecture. Firstly, training it in its recurrent form necessitates employing a backpropagation through time (BPTT) approach, which is impractical for longer sequence lengths due to its time and memory overhead. Secondly, as the hidden state $h[t]$ at time t can be a vector of floating points rather than spikes, the transition operations involved would not take complete advantage of energy/power efficient neuromorphic hardware. To achieve a fully parallelizable training procedure and leverage neuromorphic chips such as Loihi 2 during inference, we investigate an alternative formulation of Eqn.4 as a convolution

operation [11]. Since the proposed neuronal model is a time invariant system, where parameters $\overline{A}, \overline{B}, \overline{C}$ remains same over the entire sequence of input spikes X_s of length L , considering the initial hidden state before any input, i.e., $h[0]$ to be a 0-vector, the recurrent relationship can be unrolled as,

$$h[i] = \overline{A}^{i-1}\overline{B}x_s[1] + \overline{A}^{i-2}\overline{B}x_s[2] + \dots + \overline{A}\overline{B}x_s[i-1] + \overline{B}x_s[i] = \sum_{j=1}^i (\overline{A}^{i-j}\overline{B}x_s[j]) \quad (5)$$

Thus, generalizing it to the entire sequence of length L we get,

$$H = \hat{K} * X_s, \quad \hat{K} = (\overline{B}, \overline{A}\overline{B}, \dots, \overline{A}^{L-1}\overline{B}) \quad (6)$$

where, $*$ represents the non-circular convolution operation. H represents the sequence of hidden states ($h[1], h[2], \dots, h[L]$) of length L . \hat{K} is a convolutional kernel of length L as defined above. The output of the neuronal model at i^{th} step, i.e. probability of the random variable S_i is given as,

$$p_s[i] = \sigma((K * X_s)_i) \quad (7)$$

where, kernel $K = \overline{C}\hat{K} = (\overline{C}\overline{B}, \overline{C}\overline{A}\overline{B}, \dots, \overline{C}\overline{A}^{L-1}\overline{B})$; $(K * X_s)_i = \sum_{j=1}^i K_j x_s[i-j+1]$ is the i^{th} term of the non-circular convolution, where $K_i = \overline{C}\overline{A}^{i-1}\overline{B}$. $P_s = (p_s[1], p_s[2], \dots, p_s[L])$ is the sequence of probability of spikes from a neuron over the operating time steps. Thus, we can compute the output sequence parallelly by doing convolution of the input sequence of spikes with the weights of kernel K . The demonstrated sparsity of spikes, as depicted in Fig. 2, enables leveraging

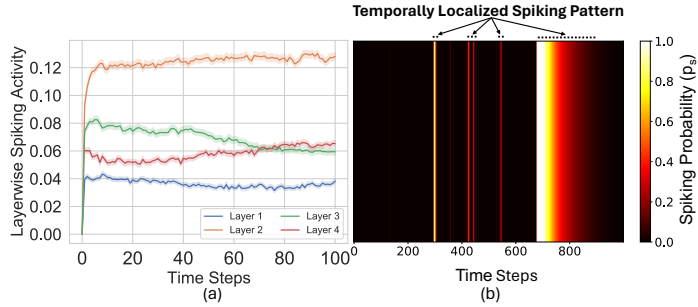


Figure 2: Results obtained after passing randomly sampled inputs from ListOps dataset of LRA benchmark through our S6-based SNN model. (a) Layer-wise spiking activity of neurons, measured as the average number of active neurons (spiking) in a layer at a particular time step, of the model is given with respect to 100 operating time steps (over 20 runs). This indicates that only 4–12% neurons in an individual layer spike at a given time step across the 4 different layers of in the model. (b) Heatmap illustrating the spiking activity over 1000 time steps of a randomly selected S6 neuron in response to a randomly sampled input.

more efficient fast-fourier transform (FFT) implementations, such as Sparse FFT [26]. This enables skipping unnecessary computations on zero elements within the input signal. Additionally, each element of the sequence P_s can be computed as a dot product of a vector of real values (elements of precomputed K) and vector of spikes (subsequence of X_s). Specialized neuromorphic hardware accelerators [27, 4] can be leveraged to perform this process sequentially, thus avoiding floating point MAC operations during inference. Furthermore, when a neuron is activated, as illustrated in the heatmap in Fig. 2b, spiking activity manifests in temporally localized patterns, mirroring the firing patterns observed in biological neurons [28], with periods of non-activity interspersed between bursts.

3.3 Scaling S6 to Deeper SNN Architectures

The current S6 neuronal model provides insight into the dynamics of individual neurons. To expand upon this foundation and construct deeper architectures, we introduce the S6 neuronal layer. This layer comprises of N S6 neurons. Alongside the S6 neuronal layer depicted in Fig. 3, we incorporate the SpikeSampler layer. This layer facilitates the sampling of spikes from the previous layer. The input to the SpikeSampler layer is clamped to $[0, 1]$ and the resultant value serves as a probability for the spike generation event. The high-level architecture of the SNN features M stacked S6 Encoder layers, each of which encapsulates the layers as shown in Fig. 3. In addition to the mentioned layer, every S6 encoder layer incorporates normalization layers and residual connections.

Neuron Mixer Layer: Since each S6 neuron independently processes input sequence tokens, a neuron mixer layer in the form of a fully-connected block is introduced. This facilitates the aggregation of spikes from previous layer of S6 neurons and efficient flow of information among neuronal layers, ensuring efficient processing of diverse temporal dependencies learned by various neurons. The operation is given as,

$$f_{mix}[t] = gelu(I_s[t] \cdot W_{fc}) \quad (8)$$

where, $I_s[t] \in \{0, 1\}^N$ are the N spikes from the previous SpikeSampler layer at time t and $W_{fc} \in \mathbb{R}^{N \times N}$ is a linear weight. We use *gelu* [29] function as a non-linearity. This layer also avoids floating point MAC operations since the input to the FC block are spikes.

We typically employ a linear layer as the encoder, with weight $W_e \in \mathbb{R}^{1 \times N}$, followed by an optional normalization layer and SpikeSampler layer. This process facilitates the generation of input spike sequences for all N neurons in the subsequent layer. This choice is informed by the prevalent structure of our datasets, wherein input data sequences are commonly formatted as $\mathbb{R}^{L \times 1}$. For classification tasks, in the final S6 encoder layer, we omit the SpikeSampler layer and use a sequence decoder to map the output of the model to the dimensionality of output labels for formulating model prediction.

Parameter Space: The S6 neuronal layer allows each of the N neurons to have their own associated parameters $\bar{A}, \bar{B}, \bar{C}$ corresponding to different individual transition dynamics. This introduces an additional level of customization to individual S6 neurons, a feature lacking in traditional SNNs. Nevertheless, we can choose to maintain an identical set of parameters for all neurons within the same layer, while allowing each layer to have its own unique set of parameters. In practice, this yields comparable accuracy to scenarios where all neuron dynamics are individually tailored, effectively mitigating increase in memory complexity within the model.

3.4 Efficient Training of deep S6 models

Surrogate Gradient: During training, S6-based SNNs encounter a non-differentiability challenge due to the SpikeSampler layer. This arises from the Bernoulli random variable S_t , at time t , which is

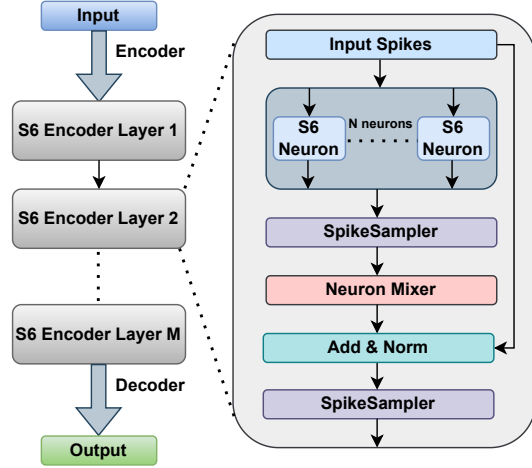


Figure 3: High-level overview of the S6-based neuronal model.

assigned a value 1 by sampling z uniformly from $[0, 1]$ and then comparing the sampled value with $p_s[t]$. If $p_s[t] < z$ then $S_t = 1$ else $S_t = 0$. To address this and enhance stability of the learning process, we propose a surrogate function (\bar{S}_t) for the stochastic spiking operation at time t as,

$$\bar{S}_t = \mathbb{E}[S_t] = 0 \cdot P(S_t = 0) + 1 \cdot P(S_t = 1) = p_s[t] \quad (9)$$

Parallel Training: This surrogate is leveraged during gradient computation for training our model. Following Eqns. 6 & 7 instead of the recurrent representation (Eqn. 4), parallel training is leveraged, thereby avoiding BPTT-based learning rule. Upon computing the kernel K , the operation involves a simple convolution of the weights given by K and the input spikes X_s . During training on GPUs, this can be effectively computed using an FFT or Sparse FFT. To efficiently compute the kernel K , we capitalize on prior theoretical structural findings regarding non-spiking SSMs [11]. By exploiting the decomposition of matrix A into a sum comprising a normal and low-rank matrix, we achieve efficient computation of K in $O(L)$ time complexity. More details regarding efficient computation of K [11] is added in the Appendix B. The state matrix (A) is initialized using HiPPO (high-order polynomial projection operators) [21] matrices $\in \mathbb{R}^{n \times n}$ and then all the parameters are updated during training.

4 Experimentation

In this section, we showcase the efficacy of our proposed S6 neuronal model-based SNN architectures by evaluating their performance across various long-range dependency based datasets. Additionally, we conduct analyses to assess net spiking activity and energy/power efficiency of our model. The experiments were run on Nvidia RTX A5000 GPUs (8) each with 24GB memory.

4.1 Permuted Sequential MNIST

To heighten the complexity of the classification task, permuted sequential MNIST (psMNIST) [34] reconfigures the presentation of images compared to the original MNIST dataset. While MNIST has each 28×28 grayscale image as a unified entity, psMNIST arranges the pixels in a sequence and in a permuted order. Thus, tackling this task demands more sophisticated models capable of effectively retaining and synthesizing information over time. A simple model comprising 2 S6 Encoder layers, each with a S6 neuronal layer consisting of 400 neurons, achieves state-of-the-art results among spiking architectures. It performs comparably to the current best non-spiking model and outperforms non-spiking transformer-based architectures, as detailed in Table 1.

4.2 Speech Command (SC10)

We use the 10-class subset of Speech Command dataset [35] following previous works [36, 11] and evaluate our model on the raw unprocessed signals of length 16000 as input. Our SNN model, featuring 4 S6 Encoder layers, each with 256 neurons, surpasses the performance of many contemporary non-spiking architectures as demonstrated in Table 2.

4.3 Long Range Arena Benchmark

To demonstrate the long-range dependency analysis capability of our S6 based architecture, we leverage the Long Range Arena (LRA) benchmark [37]. This benchmark spans various classification tasks from textual to image domains. Following are the five tasks utilized for evaluation,

Model	SNN	Acc.
S4 [11]	No	98.7
LSTM [30]	No	95.1
HSLMU [23]	Yes	96.8
LMU [31]	No	97.2
DSD-SNN [32]	Yes	97.3
Transformer [13]	No	97.9
Spiking LMUFormer [22]	Yes	97.9
TrellisNet[33]	No	98.1
HiPPO-LegS [21]	No	98.3
S6-based SNN (Our Model)	Yes	98.4

Table 1: Results comparing our model to other spiking and non-spiking architectures on test set of psMNIST dataset.

Model	SNN	Acc.
S4 [11]	No	98.3
LipschitzRNN [11]	No	×
Transformer [13]	No	×
NRDE [11]	No	16.5
Performer [20]	No	30.8
CKConv[11]	No	71.7
S6-based SNN (Our Model)	Yes	95.6

Table 2: Results comparing our model to other non-spiking architectures on test set of SC10 dataset.

Table 3: Results showing performance of our model against some spiking and non-spiking architectures on test sets of LRA benchmark tasks. Accuracy is used as the metric for all the tasks.

Model	SNN	ListOps	Text	Retrieval	Image	Pathfinder	Avg.
S4 (Original) [11]	No	58.35	76.02	87.09	87.26	86.05	80.48
S4 (Improved) [11]	No	59.60	86.82	90.90	88.65	94.20	86.09
Transformer [13]	No	36.37	64.27	57.46	42.44	71.40	54.39
Sparse Transformer[37]	No	17.07	63.58	59.59	44.24	71.71	51.24
Longformer [37]	No	35.63	62.85	56.89	42.22	69.71	53.46
Linformer [19]	No	35.70	53.94	52.27	38.56	76.34	51.36
Reformer [39]	No	37.27	56.10	53.40	38.07	68.50	50.67
Synthesizer [40]	No	36.99	61.68	54.67	41.61	69.45	52.88
BigBird [41]	No	36.05	64.02	59.29	40.83	74.87	55.01
Linear Transformer [42]	No	16.13	65.90	53.09	42.34	75.30	50.55
Performer [20]	No	18.01	65.40	53.82	42.77	77.05	51.41
Luna-256 [11]	No	37.25	64.57	79.29	47.38	77.72	59.37
Spiking LMUFormer [22]	Yes	37.30	65.80	79.76	55.65	72.68	62.24
S6-based SNN (Our Model)	Yes	55.70	77.62	88.48	80.10	83.41	77.06

- **ListOps:** In this task, our focus lies in modeling hierarchically structured data within a long-context framework. The sequence length for this task is upto $2K$.
- **Text:** In this task, we process the IMDB dataset [38] of movie reviews and perform the task of sentiment analysis in a byte-level. This is done to ensure a long sequence length of $4K$.
- **Retrieval:** In this task, we assess the model’s capacity to encode and retain compressed representations essential for matching and retrieval purposes. The input consists of byte-level sequences (of length $4K$) from two documents, and the goal is to analyze their similarity.
- **Image:** In this task, we perform an image classification task based on a sequence of pixels of the original image. The dataset is CIFAR-10 and the sequence length is $1K$.
- **Pathfinder:** In this task, we treat a 32×32 image as a sequence of pixels of length $1K$. Our objective is to make a binary decision regarding whether two points, depicted as circles, are linked by a path composed of dashes.

While the tasks in the LRA benchmark are highly relevant from a neuromorphic perspective—such as processing byte sequences for NLP and pixel sequences for image tasks—this area remains largely unexplored in neuromorphic computing. This is primarily due to two reasons: the inherent limitation in information retention capacity of vanilla LIF-based SNNs, and the scalability challenge encountered when training SNNs using BPTT (akin to an RNN) on lengthy sequence lengths. The latter issue arises from the increased memory overhead resulting from the computational graph. Moreover, transformer-based non-spiking architectures, which we use for comparison, exhibit suboptimal performance due to the overhead (while computing attention scores) associated with longer sequence lengths. In the spiking domain, we contrast our results with those of the spiking version of LMU.

Memory Footprint: Based on previous analysis [37] on LRA tasks, the Transformer models in Table 3 are configured with 4 layers, hidden dimension of 256 and 4 attention heads, resulting in approximately $600K$ parameters in total. Our models establish state-of-the-art performance in the spiking domain and comprehensively outperforms non-spiking transformer based architectures as shown in Table 3. Furthermore, considering identical parameters $(\bar{A}, \bar{B}, \bar{C})$ for neurons in the same layer, the average parameter count of our models across all five LRA tasks is around $\approx 250K$, representing a reduction of $\approx 2.4\times$ compared to the parameter count of the transformers used.

Hyper-parameters	Range	Optimal
M : #S6 Encoder Layers	(2-6)	4
N : Neurons per Layer	(64-400)	256
n : Hidden State Dim.	(4-64)	32
lr : Learning Rate	($1e-4$ - $1e-1$)	0.005
Batch Size	(8-256)	32
Epochs	20-200	50
Normalization	Batch, Layer	Batch

Table 4: Hyper-parameters for our S6-based SNN models. The optimal values are given for ListOps dataset of LRA benchmark.

4.3.1 Hyper-parameters

Initializing the state matrix A with HiPPO matrices [21] leads to optimal performance and rapid convergence. Across a majority of tasks, utilizing HiPPO-legS (further discussed in the Appendix B) consistently yields the highest accuracy. Hyper-parameters employed for training our model can be found in Table 4, with additional details in Appendix C.

4.4 Analysis of Energy Efficiency

The primary source of energy efficiency stems from the sparse neuronal activity, wherein the majority of neurons remain dormant (Fig. 4) upon encountering an input sample. Moreover, when neurons become activated, as depicted in the heatmap in Fig. 2b, the spiking activity occurs in short and temporally localized bursts with periods of no activity interspersed between bursts. By computing the spike probability $p_s[t]$ at time step t using Eqn. 7, we tap into the potential of leveraging neuromorphic hardware accelerators like Loihi 2, particularly suited for spike-based input signals. Furthermore, all operations employ accumulative (ACC) operations instead of conventional MAC operations. From a simpler circuit design perspective, ACC operations consume $5.1 \times$ less energy than MAC operations [43]. To assess the energy and power efficiency of our S6-based SNN (w.r.t a similar scale non-spiking model operation), we adopt the framework of normalized operations [44, 10]. This framework accounts for the spiking rates of each layer and their respective layer-wise operations. The total normalized OPS is defined as $Norm\#OPS = \frac{\sum_i IFR_i * Layer\#OPS_{i+1}}{\sum Layer\#OPS}$,

where IFR_i represents the total number of spikes averaged over operating time steps and the number of neurons in each layer. Consequently, the energy-efficiency factor of an SNN [10], quantified as the ratio of energy consumed by an iso-architecture ANN to that of the proposed SNN, is expressed as: $e = (\frac{1}{5.1} * Norm\#OPS)^{-1}$. For the LRA benchmark tasks (such as ListOps), the computed $Norm\#OPS$ is evaluated to be 0.17, following the sparse spiking activity pattern (Figs. 2 & 4), thus we get an $e \approx 30$. By capitalizing on the prevalence of inactive neurons and the sparse spiking patterns exhibited by active neurons, we achieve a significant improvement in energy/power efficiency on neuromorphic hardware.

5 Conclusions

Exploring the complex dynamics of biological neurons is essential for unlocking the computational ability and energy efficiency of the human brain. Our research goes beyond simplistic LIF neuronal models, aiming to create a more robust and comprehensive stochastic neuronal framework based on SSMs. Furthermore, we propose a framework to scale and efficiently train such S6-based SNN architectures. We assess the performance of our models on tasks involving long-range dependencies, such as LRA benchmark, SC10 dataset, where even non-spiking transformer architectures face challenges. Our models consistently yield state-of-the-art results for SNN-based architectures across all tested long-range dependency tasks, opening up pathways to achieve not only high performance but also exceptional energy and power efficiency through leveraging sparsity of spikes.

Limitations and Future Works: In this work, we have primarily evaluated our model on classification based long-range dependency tasks. Future work can involve using the underlying mechanism for generative tasks leveraging the S6 dynamics. Furthermore, to fully capitalize on the energy and power efficiency advantages, future next steps can consider deploying this model on edge-based devices and neuromorphic chips, such as the Intel Loihi 2.

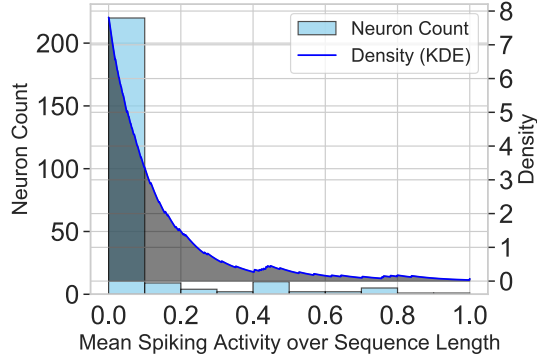


Figure 4: Results obtained after passing randomly sampled inputs from ListOps dataset of LRA benchmark through our S6-based SNN model. Figure consists of (a) Histogram representing the count of S6 neurons associated with mean probability of spiking (averaged over the entire sequence of length L), (b) Kernel density estimation (KDE) plot of the data shown in the histogram using an exponential kernel. This illustrates that over the entire sequence, majority of neurons ($\approx 90\%$) have close to 0 probability of spiking thus signifying sparse spiking pattern.

6 Acknowledgments

This material is based upon work supported in part by the U.S. National Science Foundation under award No. CCSS #2333881, EFRI BRAID #2318101, CAREER #2337646, and CCF #1955815.

References

- [1] Samanwoy Ghosh-Dastidar and Hojjat Adeli. Spiking neural networks. *International journal of neural systems*, 19(04):295–308, 2009.
- [2] Emre O Neftci, Hesham Mostafa, and Friedemann Zenke. Surrogate gradient learning in spiking neural networks: Bringing the power of gradient-based optimization to spiking neural networks. *IEEE Signal Processing Magazine*, 36(6):51–63, 2019.
- [3] Abhronil Sengupta, Yuting Ye, Robert Wang, Chiao Liu, and Kaushik Roy. Going deeper in spiking neural networks: Vgg and residual architectures. *Frontiers in neuroscience*, 13:95, 2019.
- [4] Mike Davies, Andreas Wild, Garrick Orchard, Yulia Sandamirskaya, Gabriel A Fonseca Guerra, Prasad Joshi, Philipp Plank, and Sumedh R Risbud. Advancing neuromorphic computing with loihi: A survey of results and outlook. *Proceedings of the IEEE*, 109(5):911–934, 2021.
- [5] Paul A Merolla, John V Arthur, Rodrigo Alvarez-Icaza, Andrew S Cassidy, Jun Sawada, Filipp Akopyan, Bryan L Jackson, Nabil Imam, Chen Guo, Yutaka Nakamura, et al. A million spiking-neuron integrated circuit with a scalable communication network and interface. *Science*, 345(6197):668–673, 2014.
- [6] Anthony N Burkitt. A review of the integrate-and-fire neuron model: I. homogeneous synaptic input. *Biological cybernetics*, 95:1–19, 2006.
- [7] AL Hodgkin and AF Huxley. A quantitative description of membrane current and its application to conduction and excitation in nerve. *Bulletin of mathematical biology*, 52:25–71, 1990.
- [8] LM Harrison, O David, and KJ Friston. Stochastic models of neuronal dynamics. *Philosophical Transactions of the Royal Society B: Biological Sciences*, 360(1457):1075–1091, 2005.
- [9] Zhaokun Zhou, Yuesheng Zhu, Chao He, Yaowei Wang, Shuicheng Yan, Yonghong Tian, and Li Yuan. Spikformer: When spiking neural network meets transformer. *arXiv preprint arXiv:2209.15425*, 2022.
- [10] Malyaban Bal and Abhronil Sengupta. Spikingbert: Distilling bert to train spiking language models using implicit differentiation. In *Proceedings of the AAAI Conference on Artificial Intelligence*, volume 38, pages 10998–11006, 2024.
- [11] Albert Gu, Karan Goel, and Christopher Ré. Efficiently modeling long sequences with structured state spaces. *arXiv preprint arXiv:2111.00396*, 2021.
- [12] Albert Gu and Tri Dao. Mamba: Linear-time sequence modeling with selective state spaces. *arXiv preprint arXiv:2312.00752*, 2023.
- [13] Ashish Vaswani, Noam Shazeer, Niki Parmar, Jakob Uszkoreit, Llion Jones, Aidan N. Gomez, Lukasz Kaiser, and Illia Polosukhin. Attention is all you need, 2017.
- [14] Mollie Ward and Oliver Rhodes. Beyond lif neurons on neuromorphic hardware. *Frontiers in Neuroscience*, 16:881598, 2022.
- [15] Christian Mayr, Sebastian Hoepfner, and Steve Furber. Spinnaker 2: A 10 million core processor system for brain simulation and machine learning. *arXiv preprint arXiv:1911.02385*, 2019.
- [16] Tianyuan Yu, Yongxin Yang, Da Li, Timothy Hospedales, and Tao Xiang. Simple and effective stochastic neural networks. In *Proceedings of the AAAI Conference on Artificial Intelligence*, volume 35, pages 3252–3260, 2021.

- [17] Yi Jiang, Sen Lu, and Abhronil Sengupta. Stochastic spiking neural networks with first-to-spike coding. *arXiv preprint arXiv:2404.17719*, 2024.
- [18] Jianchuan Ding, Bo Dong, Felix Heide, Yufei Ding, Yunduo Zhou, Baocai Yin, and Xin Yang. Biologically inspired dynamic thresholds for spiking neural networks. *Advances in Neural Information Processing Systems*, 35:6090–6103, 2022.
- [19] Sinong Wang, Belinda Z Li, Madian Khabsa, Han Fang, and Hao Ma. Linformer: Self-attention with linear complexity. *arXiv preprint arXiv:2006.04768*, 2020.
- [20] Krzysztof Choromanski, Valerii Likhoshesterov, David Dohan, Xingyou Song, Andreea Gane, Tamas Sarlos, Peter Hawkins, Jared Davis, Afroz Mohiuddin, Lukasz Kaiser, et al. Rethinking attention with performers. *arXiv preprint arXiv:2009.14794*, 2020.
- [21] Albert Gu, Tri Dao, Stefano Ermon, Atri Rudra, and Christopher Ré. Hippo: Recurrent memory with optimal polynomial projections. *Advances in neural information processing systems*, 33:1474–1487, 2020.
- [22] Zeyu Liu, Gourav Datta, Anni Li, and Peter Anthony Beerel. Lmuformer: Low complexity yet powerful spiking model with legendre memory units. *arXiv preprint arXiv:2402.04882*, 2024.
- [23] Aaron R Voelker, Daniel Rasmussen, and Chris Eliasmith. A spike in performance: Training hybrid-spiking neural networks with quantized activation functions. *arXiv preprint arXiv:2002.03553*, 2020.
- [24] Yu Du, Xu Liu, and Yansong Chua. Spiking structured state space model for monaural speech enhancement. In *ICASSP 2024-2024 IEEE International Conference on Acoustics, Speech and Signal Processing (ICASSP)*, pages 766–770. IEEE, 2024.
- [25] Arnold Tustin. A method of analysing the behaviour of linear systems in terms of time series. *Journal of the Institution of Electrical Engineers-Part IIA: Automatic Regulators and Servo Mechanisms*, 94(1):130–142, 1947.
- [26] Haitham Hassanieh, Piotr Indyk, Dina Katabi, and Eric Price. Simple and practical algorithm for sparse fourier transform. In *Proceedings of the twenty-third annual ACM-SIAM symposium on Discrete Algorithms*, pages 1183–1194. SIAM, 2012.
- [27] Dmitry Ivanov, Aleksandr Chezhegov, and Denis Larionov. Neuromorphic artificial intelligence systems. *Frontiers in Neuroscience*, 16:959626, 2022.
- [28] David H Hubel and Torsten N Wiesel. Receptive fields, binocular interaction and functional architecture in the cat’s visual cortex. *The Journal of physiology*, 160(1):106, 1962.
- [29] Dan Hendrycks and Kevin Gimpel. Gaussian error linear units (gelus). *arXiv preprint arXiv:1606.08415*, 2016.
- [30] Albert Gu, Caglar Gulcehre, Thomas Paine, Matt Hoffman, and Razvan Pascanu. Improving the gating mechanism of recurrent neural networks. In *International Conference on Machine Learning*, pages 3800–3809. PMLR, 2020.
- [31] Aaron Voelker, Ivana Kajić, and Chris Eliasmith. Legendre memory units: Continuous-time representation in recurrent neural networks. *Advances in neural information processing systems*, 32, 2019.
- [32] Bing Han, Feifei Zhao, Yi Zeng, Wenxuan Pan, and Guobin Shen. Enhancing efficient continual learning with dynamic structure development of spiking neural networks. *arXiv preprint arXiv:2308.04749*, 2023.
- [33] Shaojie Bai, J Zico Kolter, and Vladlen Koltun. Trellis networks for sequence modeling. *arXiv preprint arXiv:1810.06682*, 2018.
- [34] Quoc V Le, Navdeep Jaitly, and Geoffrey E Hinton. A simple way to initialize recurrent networks of rectified linear units. *arXiv preprint arXiv:1504.00941*, 2015.

- [35] Pete Warden. Speech commands: A dataset for limited-vocabulary speech recognition. *arXiv preprint arXiv:1804.03209*, 2018.
- [36] Patrick Kidger, James Morrill, James Foster, and Terry Lyons. Neural controlled differential equations for irregular time series. *Advances in Neural Information Processing Systems*, 33: 6696–6707, 2020.
- [37] Yi Tay, Mostafa Dehghani, Samira Abnar, Yikang Shen, Dara Bahri, Philip Pham, Jinfeng Rao, Liu Yang, Sebastian Ruder, and Donald Metzler. Long range arena: A benchmark for efficient transformers. *arXiv preprint arXiv:2011.04006*, 2020.
- [38] Andrew Maas, Raymond E Daly, Peter T Pham, Dan Huang, Andrew Y Ng, and Christopher Potts. Learning word vectors for sentiment analysis. In *Proceedings of the 49th annual meeting of the association for computational linguistics: Human language technologies*, pages 142–150, 2011.
- [39] Nikita Kitaev, Łukasz Kaiser, and Anselm Levskaya. Reformer: The efficient transformer. *arXiv preprint arXiv:2001.04451*, 2020.
- [40] Yi Tay, Dara Bahri, Donald Metzler, D Juan, Zhe Zhao, and Che Zheng. Synthesizer: Rethinking self-attention in transformer models. arxiv 2020. *arXiv preprint arXiv:2005.00743*, 2, 2020.
- [41] Manzil Zaheer, Guru Guruganesh, Kumar Avinava Dubey, Joshua Ainslie, Chris Alberti, Santiago Ontanon, Philip Pham, Anirudh Ravula, Qifan Wang, Li Yang, et al. Big bird: Transformers for longer sequences. *Advances in neural information processing systems*, 33: 17283–17297, 2020.
- [42] Angelos Katharopoulos, Apoorv Vyas, Nikolaos Pappas, and François Fleuret. Transformers are rnns: Fast autoregressive transformers with linear attention. In *International conference on machine learning*, pages 5156–5165. PMLR, 2020.
- [43] Song Han, Jeff Pool, John Tran, and William J. Dally. Learning both weights and connections for efficient neural networks, 2015.
- [44] Sen Lu and Abhronil Sengupta. Exploring the connection between binary and spiking neural networks. *Frontiers in neuroscience*, 14:535, 2020.

A Deriving Convolutional Representation of S6 Neuronal Dynamics

At time step t , the discretized S6 neuronal model exhibits transition dynamics described as follows:

$$\begin{aligned} h[t] &= \overline{A}h[t-1] + \overline{B}x_s[t] \\ p_s[t] &= \sigma(\overline{C}h[t]) \end{aligned} \quad (\text{S1})$$

where, $h[t]$ is the hidden state of the neuron, $p_s[t]$ is the probability of the spiking event S_t . \overline{A} , \overline{B} , \overline{C} are the discretized parameters of the time-invariant system. Considering at time step 0, $h[0] = 0$, we get,

$$\begin{aligned} h[1] &= \overline{B}x_s[1] \\ h[2] &= \overline{A}\overline{B}x_s[1] + \overline{B}x_s[2] \end{aligned} \quad (\text{S2})$$

Unrolling like this to time step i we get,

$$h[i] = \overline{A}^{i-1}\overline{B}x_s[1] + \overline{A}^{i-2}\overline{B}x_s[2] + \dots + \overline{A}\overline{B}x_s[i-1] + \overline{B}x_s[i] = \sum_{j=1}^i (\overline{A}^{i-j}\overline{B}x_s[j]) \quad (\text{S3})$$

Thus, the convolutional kernel \hat{K} , whose length is given by the length of the input sequence L , is defined as,

$$\hat{K} = (\overline{B}, \overline{A}\overline{B}, \dots, \overline{A}^{L-1}\overline{B}) \quad (\text{S4})$$

Now H , i.e., sequence of hidden states can be computed as a non-circular convolution given as, $H = \hat{K} * X_s$, where X_s is the input sequence of spikes.

Thus, $p_s[t] = \sigma((K * X_s)_t) = \sigma(\sum_{j=1}^t K_j x_s[t-j+1])$, where $K = (\overline{C}\overline{B}, \overline{C}\overline{A}\overline{B}, \dots, \overline{C}\overline{A}^{L-1}\overline{B})$.

B HiPPO-legS Matrix

HiPPO (high-order polynomial projection operators) [21] is a versatile framework that enables the analysis of various families of measures. Utilizing this operator as either a closed-form ordinary differential equation (ODE) or a linear recurrence, we can efficiently update the optimal polynomial approximation as the input function unfolds over time. HiPPO-legS can generalize to different time scales. HiPPO enables the hidden state to effectively memorize the historical pattern of input spikes (in our paper). The elements of the HiPPO-legS (Scaled Legendre) matrix $\in \mathbb{R}^{n \times n}$ is given below,

$$A_{mk} = - \begin{cases} \sqrt{2m+1}\sqrt{2k+1}, & \text{if } m > k \\ m+1, & \text{if } m = k \\ 0, & \text{if } m < k \end{cases} \quad (\text{S5})$$

B.1 Computing Kernel K

The efficient computation of K has been proposed in the literature [11], thus speeding up the parallel training of the SSM based neuronal architectures. We briefly go over the overview on how it is achieved. The primary concern in computing K is the repeated multiplication of the state matrix to create the individual terms K_i . Thus to compute K , the time complexity for a simple approach of chained multiplication is $O(n^2L)$, where n is the hidden state dimension and L is the sequence length. Now the idea is that, if we had the state matrix to be a diagonal matrix, then theoretically we could compute K efficiently using Vandermonde product. Thus, the goal is to diagonalize the matrix A . Now, the ideal scenario is if A is a normal matrix, i.e., it is diagonalizable with a unitary matrix (UAU^{-1} is a diagonal matrix, where U is a square matrix such that $U^H = U^{-1}$). A is initialized to HiPPO matrices which are not normal matrices. However, HiPPO can be decomposed into a diagonal matrix (Λ) and a low-rank matrix. Following this, we can leverage previous theoretical results [11]

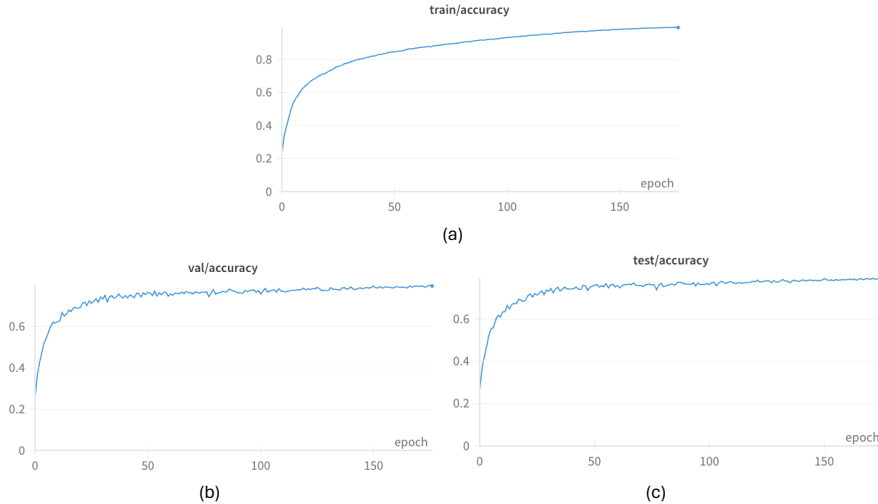


Figure S1: Experiments run on the LRA: Image dataset with sequence length $1K$. (a) Train accuracy vs epochs. (b) Validation accuracy vs epochs. (c) Test accuracy vs epochs.

Dataset	Accuracy
psMNIST	98.3 ± 0.1
SC10	95.4 ± 0.2
LRA: ListOpns	55.5 ± 0.2
LRA: Text	77.3 ± 0.3
LRA: Retrieval	88.3 ± 0.1
LRA: Image	80.0 ± 0.1
LRA: Pathfinder	83.2 ± 0.2

Table S1: Accuracy statistics across different datasets.

on reducing the underlying SSM to the computation of Cauchy kernels and calculate K , in linear order of time complexity w.r.t the sequence length L .

C Additional Experimental Results

In Table S2, we list the optimal set of hyper-parameters used for each of the tasks. Primarily batch normalization was used for normalization. As mentioned in the main text, the state matrix A is initialized to the HiPPO-legS matrix as shown in Eqn. S3. The step size for discretization (Δ) is restricted between $[0.001, 0.1]$. The comprehensive statistics of accuracy obtained after running 10 different instances of each experiment with random seeds is shown in Table S1. We also demonstrate the train/test/validation convergence graph with respect to epochs run of the LRA: Image dataset in Fig. S1. In the 175 epochs shown in the graph, the train accuracy reaches above 99%, while the validation and test accuracy is $> 80\%$. The memory footprint ranges from $\approx 6GB$ for psMNIST to $\approx 23GB$ for SC10. The dataset splits are aligned with prior literature [37].

Table S2: Hyper-parameters used for obtaining the best result on individual datasets used for evaluating S6-based SNN models.

	psMNIST	SC10	ListOpns	Text	Retrieval	Image	Pathfinder
M : #S6 Encoder Layers	2	4	4	4	4	4	4
N : Neurons per Layer	400	256	256	256	200	256	256
n : Hidden State Dim.	64	32	32	16	32	32	64
lr : Learning Rate	0.01	0.002	0.005	0.0005	0.003	0.005	0.0005
Batch Size	64	32	32	64	32	32	32
Epochs	100	50	50	80	50	150	150